Acta Crystallographica Section D
Biological Crystallography
ISSN 0907-4449

Cloning, expression and preliminary crystallographic studies of the potential drug target purine nucleoside phosphorylase from *Schistosoma mansoni*

Humberto M. Pereira,[a]* Anne Cleasby,[b] Sérgio D. J. Pena,[c] Glória R. Franco[c] and Richard C. Garratt[a]

[a]Instituto de Física de São Carlos, Universidade de São Paulo, Brazil, [b]Astex Technology, Cambridge, England, and [c]Departamento de Bioquímica e Imunologia, Instituto de Ciências Biologicas, UFMG, Brazil

Correspondence e-mail: hmuniz@if.sc.usp.br

Received 28 January 2003
Accepted 7 April 2003

The parasite *Schistosoma mansoni*, unlike its mammalian hosts, lacks the *de novo* pathway for purine biosynthesis and depends on salvage pathways for its purine requirements. The gene encoding one enzyme of this pathway, purine nucleoside phosphorylase from *S. mansoni* (SmPNP) was identified, fully sequenced and cloned into the bacterial expression vector pMAL c2G to produce a protein in fusion with maltose-binding protein. The recombinant fusion protein was expressed at high levels and was purified in a single step by amylose resin affinity chromatography. After factor Xa cleavage, SmPNP was purified using a cation-exchange column and crystallized by hanging-drop vapour diffusion using polyethylene glycol 1500 as precipitant in the presence of 20% glycerol in acetate buffer. The use of the non-detergent sulfobetaine 195 (NDSB 195) as an additive had a marked effect on the size of the resulting crystals. Two data sets were obtained, one from a crystal grown in the absence of NDSB 195 and one from a crystal grown in its presence. The crystals are isomorphous and belong to the space group $P2_12_12_1$. It is intended to use the structures in the discovery and development of specific inhibitors of SmPNP.

1. Introduction

Schistosomiasis is a major public health problem in the developing world. It is endemic in 76 countries and territories and amongst the parasitic diseases ranks second after malaria in terms of social and economic impact and public health importance (Shuhua *et al.*, 2002). The World Health Organization estimates that in 1999, 652 million people were at risk from the disease, with 193 million actually infected (World Health Organization, 1999). The disease is caused by a trematode parasite (blood fluke) or schistosome, of which the principal species is *Schistosoma mansoni*.

The *Schistosoma* Genome Project was created in 1992 to encourage research in strategic areas, especially those that will lead to the discovery and development of new drugs and vaccines. The main objectives were (i) the discovery and characterization of new genes from *S. mansoni* and *S. japonicum*, (ii) the development of a low-resolution physical map, (iii) the sequencing and analysis of the mitochondrial genome, (iv) the development of new resources to be used and distributed and (v) the construction and maintenance of a WWW site, the ShistoDB (Franco *et al.*, 2000).

As part of this project (Franco *et al.*, 1995), we have identified and isolated the gene coding for the enzyme purine nucleoside phosphorylase from an adult worm cDNA library, which we named SmPNP (*S. mansoni* PNP). Purine nucleoside phosphorylase (PNP; EC 2.4.2.1) catalyzes the reversible phosphorolysis of purine nucleosides to generate the corresponding purine base and ribose 1-phosphate and has previously been described as participating in the purine-salvage pathway in *S. mansoni* (Senft & Crabtree, 1977).

It has been demonstrated that schistosomes (Senft & Crabtree, 1983) and their larvae shistosomules (Dovey *et al.*, 1984), unlike their mammalian hosts, do not have the capacity to synthesize purine nucleosides *de novo* and depend exclusively upon the salvage pathway for their purine requirements, suggesting that the pathway's component enzymes may represent potential drug targets for novel chemotherapy. Indeed, the purine-salvage pathway has been successfully exploited as a drug target against several other parasites in the past by the use of purine and purine nucleoside analogues (Nelson *et al.*, 1979; Carlson & Chang, 1981) and may therefore also be useful in the development of novel compounds for the combat of schistosomiasis.

More recently, interest in the salvage pathway has been rekindled and it has been suggested that selective inhibitors of PNP from parasites could prevent the spread of parasitic infections (Bzowska *et al.*, 2000). For example, Immucillin-H, a transition-state analogue of PNP, is a potent inhibitor of the enzyme from *Plasmodium falciparum*, thus preventing the utilization of inosine and deoxyinosine as a

source of hypoxanthine. This indicates that PNP may be a viable target for antimalarial therapy (Kicska *et al.*, 2002).

A further reason for investing in a PNP-based drug-design strategy is the fact that it has been intensively studied as a target for other diseases. For example, potent inhibitors of PNPs may also be useful as immunosuppressive agents as well as in the treatment of gout and in the enhancement of the therapeutic effects of drugs that are purine nucleosides and are therefore cleaved by PNP prior to reaching their target (Koellner *et al.*, 1997). It is to be expected that the crystallographic structure of SmPNP will help in the search for and/or development of compounds that inhibit *S. mansoni* PNP specifically and that could be useful in the treatment of schistosomiasis in the future.

2. Material and methods

2.1. Cloning, expression and purification of SmPNP

SmPNP cDNA was identified and partially sequenced as part of the *S. mansoni* Genome Project (Franco *et al.*, 1995). Both strands of the gene were subsequently sequenced using the Automated Fluorescent DNA Sequencer (Amersham Biosciences), making use of a restriction-enzyme digestion and subcloning strategy for full coverage of the cDNA. The 973 bp SmPNP cDNA was amplified by PCR using two oligonucleotides: Smpnp1, 5′-CTG**GGATCC***ATCGAGGGAAGG*ATGCATGAGTCAGTAACT-3′, including a cleavage site for factor Xa protease (in italics) inserted before the ATG initiation codon, as well as a *Bam*HI restriction site (in bold), and Smpnp2, 5′-CTG**CTGCAG**TAGACAGAAAACTTTATAAG-3′, including a *Pst*1 restriction site (in bold). The amplified SmPNP cDNA was inserted into the pMAL c2G vector (New England Biolabs) fused to that of the maltose-binding protein (MBP) and the fusion plasmid was used in the transformation of DH5α. Expression of the corresponding fusion protein was performed in 1 l 2×YT medium in the presence of 100 µg ml^{-1} ampicillin and 2% glucose, inoculated with an overnight culture. The cells were incubated at 310 K to an OD_{600} of about 0.6 and induced with 300 µ*M* of isopropyl β-D-thiogalactopyranoside (IPTG) for 2.5 h. The culture was harvested by centrifugation and sonicated in an ice bath. After centrifugation, the crude extract was applied to an amylose affinity column and the fusion protein was eluted with 10 m*M* maltose. The fusion protein was cleaved with factor Xa (1 U per 200 µg of fusion protein) for 4 d at 277 K. The cleavage product was dialyzed against 20 m*M* MES pH 6.0 and the SmPNP was then purified by cation-exchange chromatography on a Poros 20SP (4.6 × 100 mm) or a Mono-S column (Amersham Biosciences) using a linear gradient of 0–1 *M* NaCl. All stages of SmPNP production were visualized by SDS–PAGE. Fractions containing the purified enzyme were pooled, dialyzed against 10 m*M* β-mercaptoethanol and concentrated to about 12 mg ml^{-1} by ultrafiltration (Centriprep YM-10).

2.2. Enzyme assay

The inosine phosphorolysis activity of SmPNP was assayed by the coupled xanthine oxidase method of Kalckar (1947). This method consists of measurement of the hypoxanthine released during phosphorolysis of inosine or deoxyinosine indirectly by monitoring the uric acid produced by xanthine oxidase on its oxidation. The standard reaction mixture (final volume 1 ml) contained 50 m*M* potassium phosphate buffer pH 7.4, 5–250 µ*M* inosine and 0.02 units of xanthine oxidase. The reaction was started by addition of 350 ng of SmPNP to the reaction mixture and the OD_{293} was immediately monitored with a UV–Vis spectrophotometer. The kinetic parameters (K_M and k_{cat}) were derived from non-linear least-squares fits of the Michaelis–Menten equation using the experimental data.

2.3. Crystallization

SmPNP crystallization was performed by the hanging-drop vapour-diffusion method at 277 K. The initial crystallization condition obtained was solution 43 from Crystal Screen Cryo (Hampton Research), which consists of 24% PEG 1500 and 20% glycerol. Refinement of this condition was performed by varying the pH by including different buffers (32 m*M* Tris–HCl pH 8.0, 7.5 and 7.0, 32 m*M* cacodylic acid pH 6.0 and 32 m*M* sodium acetate pH 5.6, 5.3, 5.0 and 4.0). SmPNP crystals only appeared in sodium acetate buffer pH 5.0 and therefore a second optimization was performed using a finer pH grid with 32 m*M* sodium acetate buffer pH 4.8–5.5 in pH increments of 0.1. The final optimized condition was 24% PEG 1500, 20% glycerol pH 4.9–5.0. The hanging drop (4 µl) contained 2 µl of SmPNP solution at 10–12 mg ml and 2 µl of well solution and was equilibrated against 500 µl of well solution. Improvements in the crystal size were obtained using the non-detergent sulfobetaine 195 (NDSB 195; Vuillard *et al.*, 1996) as an additive and an SmPNP concentration reduced to 9 mg ml^{-1}. In this case, it was necessary to increase the PEG 1500 concentration to 28–30% and NDSB195 was included in the SmPNP solution at a final concentration of 600 m*M*. The same drop size was used as described above.

2.4. X-ray data collection and processing

SmPNP crystals were always grown in the presence of the cryoprotectant glycerol and two separate data sets were collected. The first originated from a small crystal grown in the absence of NDSB 195. This crystal was mounted in a nylon-fibre loop and flash-frozen in liquid nitrogen. Diffraction data were measured at 100 K using synchrotron radiation on beamline CPr at the Laboratório Nacional de Luz Síncrotron (LNLS, Campinas, Brazil) and copper-like radiation (λ = 1.544). Diffraction data were collected to 2.75 Å resolution using 1° φ increments over a total rotation of 95°. The data were indexed, integrated and scaled using the *HKL* program package (Otwinowski & Minor, 1997). A second data set from a crystal grown in the presence of NDSB 195 was collected on beamline ID 14.1 of the ESRF using λ = 0.993 at 100 K. Diffraction data were collected to 1.75 Å resolution using 0.5° φ increments over a total rotation of 90°. The data were indexed and integrated using the program *MOSFLM* (Leslie, 1992) and scaled using the program *SCALA* from the *CCP*4 suite (Collaborative Computational Project, Number 4, 1994).

2.5. Molecular replacement

The first molecular replacement of SmPNP was performed using the program *AMoRe* (Navaza, 1994) using the data collected to 2.75 Å resolution. The crystal structure of trimeric bovine PNP (PDB code 4pnp) was used as the search model using all data in the resolution range 15–3.5 Å and an integration radius of 45.59 Å. For the data collected to 1.75 Å resolution, molecular replacement was performed using the program *MOLREP* (Vagin & Teplyakov, 1997; Vaguine *et al.*, 1999) as implemented in the *CCP*4 program package (Collaborative Computational Project, Number 4, 1994). The partially refined SmPNP trimer was used as the search model in this case using all data in the resolution range 45.0–3.0 Å and an integration radius of 27.0 Å.

```
Smpnp     MHESVTANIENVKKVAHHIQKLTSIVPEIGIICGSGLGKLADGVKDKITIPYTKIPNFPQ 60
HuPNP     MENGYT--YEDYKNTAEWLLSHTKHRPQVAIICGSGLGGLTDKLTQAQIFDYSEIPNFPR 58
BovPNP    MANGYT--YEDYQDTAKWLLSHTEQRPQVAVICGSGLGGLVNKLTQAQTFDYSEIPNFPE 58
          *    *   *     *      *   *    ******* *          *  *****

Smpnp     TSVVGHSGNLIFGTLSGRKVVVMQGRFHMYEGYSNDTVALPIRVMKLLGVKILMVSNAAG 120
HuPNP     STVPGHAGRLVFGFLNGRACVMMQGRFHMYEGYPLWKVTFPVRVFHLLGVDTLVVTNAAG 118
BovPNP    STVPGHAGRLVFGILNGRACVMMQGRFHMYEGYPFWKVTFPVRVFRLLGVETLVVTNAAG 118
            * ** * * ** * **  * ***********    *  * **  ****  * * ****

Smpnp     GLNRSLKLGDFVILKDHIYLPGLGLNNILVGPNQEAFGTRFPALSNAYDRDLRKLAVQVA 180
HuPNP     GLNPKFEVGDIMLIRDHINLPGFSGQNPLRGPNDERFGDRFPAMSDAYDRTMRQRALSTW 178
BovPNP    GLNPNFEVGDIMLIRDHINLPGFSGENPLRGPNEERFGVRFPAMSDAYDRDMRQKAHSTW 178
          ***     **     *** ***    * * *** * ** **** * ****  *  *

Smpnp     EKNGFGNLVHQGVYVMNGGPCYETPAECTMLLNMGCDVVGMSTIPEVVIARHCGIQVFAV 240
HuPNP     KQMGEQRELQEGTYVMVAGPSFETVAECRVLQKLGADAVGMSTVPEVIVARHCGLRVFGF 238
BovPNP    KQMGEQRELQEGTYVMLGGPNFETVAECRLLRNLGADAVGMSTVPEVIVARHCGLRVFGF 238
             *       * ***  **  ** ***  *   * * ***** ***  *****  **

Smpnp     SLVTNISVLDVESDLKPNHEEVLATGAQRAELMQSWFEKIIEKLPKD---- 287
HuPNP     SLITNKVIMDYESLEKANHEEVLAAGKQAAQKLEQFVSILMASIPLPDKAS 285
BovPNP    SLITNKVIMDTESQGKANHEEVLEAGKQAAQKLEQFVSLLMASIPVSGHTG 285
          ** **    * **  * ******  * * *
```

Figure 1
Sequence alignment of SmPNP, human and bovine PNPs. The conserved residues are marked with asterisks. The residues of the active site are underlined and the two mutations in the active site are highlighted.

3. Results and discussion

3.1. Sequence comparison, purification and activity assay

The open reading frame corresponding to the SmPNP gene is 864 bp in length, coding for a 287-residue protein with a calculated molecular mass of 31 162.2 Da. This compares with 31 166.6 Da as determined for the purified enzyme by electrospray mass spectrometry. The difference is probably within the experimental error of the mass spectrometry or owing to uncertainty in the protonation states of ionizable residues. A BLAST search showed that SmPNP is most similar to the mammalian PNPs and an alignment of the parasite enzyme with human and bovine homologues (Williams *et al.*, 1984; Bzowska *et al.*, 1995) is shown in Fig. 1. In both cases, SmPNP presents 49% sequence identity. These data clearly classify SmPNP as a member of the low-molecular-mass PNPs, which are homotrimers with an M_r of between 80 and 100 kDa that are specific for the catalysis of 6-oxopurines and their nucleosides (Bzowska *et al.*, 2000).

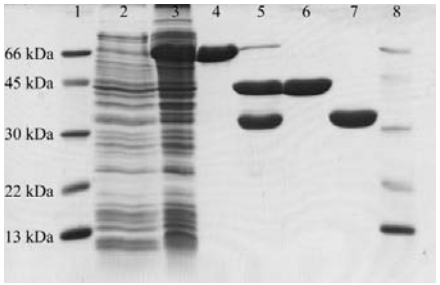

Figure 2
Analysis of the purification of SmPNP by 15% SDS–PAGE after Coomassie blue staining. Lanes 1 and 8 are markers containing serum bovine albumin (66 kDa), ovalbumin (45 kDa), carbonic anhydrase (30 kDa), trypsin inhibitor (22.4 kDa), cytochrome *c* (13.4 kDa). Lane 2, crude bacterial lysates prior to IPTG induction; lane 3, crude bacterial lysates after 0.3 m*M* IPTG induction for 2.5 h; lane 4, purified fusion protein (MBP-SmPNP) after amylose affinity column chromatography; lane 5, the result of cleavage of the fusion protein with factor Xa; lane 6, MBP eluted in the void volume on Poros 20SP column chromatography; lane 7, purified SmPNP after elution from the Poros 20SP with an NaCl gradient.

The N- and C-termini show low sequence identity when compared with the human and bovine homologues. Furthermore, despite conservation of the phosphate and ribose-1-phosphate binding subsites (underlined residues in Fig. 1), two mutations are observed in the base-binding subsite of the active site. Phe200 and Lys244 in the human and bovine enzymes are replaced by Tyr202 and Ile246 in SmPNP, respectively. These differences suggest the real possibility of designing nucleoside-based inhibitors which are sufficiently selective to be useful anti-parasitic agents. They represent the principal stimulus behind investing further effort in structural studies.

The primer Smpnp1 inserted a factor Xa cleavage site between MBP and SmPNP. The use of factor Xa protease has the advantage of producing a protein product with no additional residues at the N-terminus. This may be critical in cases where the N-terminus is expected to be buried or close to an interface between subunits, as is the case for trimeric PNPs. Indeed, previous attempts to crystallize an SmPNP product which included ten extra N-terminal residues derived from the vector were systematically unsuccessful.

Each purification step was monitored by SDS–PAGE (Fig. 2). Typically, 80 mg of recombinant fusion protein were obtained from 1 l of cell culture. After cleavage of 30 mg of this fusion protein using factor Xa, approximately 8 mg of SmPNP were obtained. The gel shows the remarkable efficiency of the cleavage (lane 5) both in terms of yield and a total lack of side products resulting from non-specific proteolysis.

Kinetic studies showed that the recombinant SmPNP is active against inosine, with a K_M of 7 μ*M* and a k_{cat} of 1.78 s^{-1}. These values are roughly comparable with those published for the human enzyme (45 μ*M* and 57 s^{-1}; Stoeckler *et al.*, 1997), but show a slightly greater apparent substrate affinity compensated by a reduced turnover rate. The significance, if any, of these differences for parasite metabolism has yet to be evaluated and their structural basis must await full refinement of SmPNP to high resolution.

3.2. Crystallization, preliminary X-ray analysis and molecular replacement

Crystals obtained in the absence of the additive NDSB 195 grew to 0.15 mm in the largest dimension and were obtained using 32 m*M* sodium acetate buffer pH 4.9–5.0, 24% PEG 1500 and 20% glycerol. These crystals took approximately three weeks to reach their full size. On the other hand, much larger crystals (up to 0.6 mm in the largest dimension) were obtained after only 3 d in the presence of 600 m*M* NDSB 195. These crystals were obtained under essentially identical conditions to those described above but in the presence of a slightly increased precipitant concentration, 28–30% PEG 1500 (Fig. 3).

Data sets were collected from crystals grown under both conditions. The use of NDSB 195 in the crystallization clearly resulted in several improvements to the crystals obtained: (i) they grew more rapidly, attaining their full size after a maximum of 3 d compared with three weeks in the absence of the additive, (ii) the final size obtained was at least four times greater in all dimensions and (iii) the resolution of the crystals improved from 2.75 to 1.75 Å. Although in the latter case it is difficult to make direct comparisons between the two data sets as different radiation sources and wavelengths were used, we presume that the increased size of the crystals and the improvement in resolution are both manifestations of a greater internal order. The

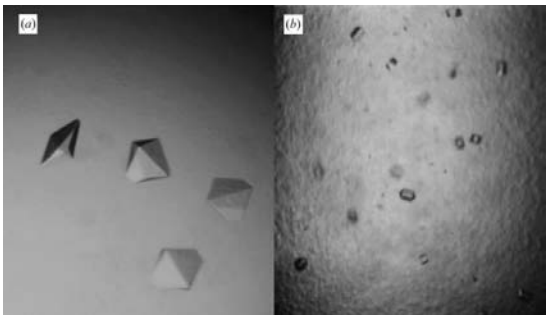

Figure 3
Crystals of SmPNP grown in (*a*) the presence and (*b*) the absence of NDSB 195.

Table 1
X-ray data-collection and processing statistics.

Values in parentheses correspond to the highest resolution shell.

Crystal form	Without NDSB 195	With NDSB 195
Space group	$P2_12_12_1$	$P2_12_12_1$
Unit-cell parameters (Å)		
a	47.30	48.75
b	119.19	122.06
c	130.94	129.76
Resolution range (Å)	20.0–2.75 (2.81–2.75)	45.0–1.75 (1.83–1.75)
V_M (trimer per AU) ($Å^3\,Da^{-1}$)	1.97	2.06
Solvent content (%)	37.24	39.96
Unique reflections	19240 (1244)	78422 (11027)
R_{merge} (%)	8.0 (27.9)	8.1 (29.8)
Completeness	96.5 (95.0)	99.3 (97.1)
Average $I/\sigma(I)$	8.6 (3.1)	4.7 (2.5)

crystals are isomorphous and belong to space group $P2_12_12_1$. Analysis of crystals grown in the absence of the additive suggests a trimer in the asymmetric unit (V_M = 1.97 $Å^3\,Da^{-1}$), corresponding to a solvent content of 37.24%. Alterations in the unit-cell parameters between the two crystal forms vary from 3.1% in *a* to 1.0% in *c*, corresponding to a total unit-cell volume increase of 4.5% for the crystals grown in the presence of NDSB 195 (Table 1).

Non-detergent sulfobetaine solubilizers/stabilizers such as NDSB 195 are believed to act principally by increasing the solubility and stability of the protein and consequently leading to a reduction in non-specific aggregation (Vuillard *et al.*, 1996). As a result, this favours the formation of appropriate crystal contacts, leading to improved crystal growth. This increased solubility probably explains why a slightly greater precipitant concentration was necessary for crystallization in the presence of the additive (from 24% to 28–30%). The sulfobetaine itself, however, may not be visible in the final electron-density map. In the present case, an explanation for the its effects in improving crystal-growth rate, size and quality must await full structure refinement.

In the case of the crystals grown in the absence of NDSB 195, a unique molecular-replacement solution was obtained with a correlation coefficient of 33% and an *R* factor of 45%. Despite the relatively poor molecular-replacement solution, electron-density maps were calculated using the program *CNS* (Brünger *et al.*, 1998) and these, together with the resulting crystal packing, demonstrated the solution to be correct. A partially refined SmPNP structure resulting from this solution was used as the search model for the crystals obtained in the presence of the additive and yielded a correlation coefficient of 70.7% and an *R* factor of 34.7%. The solution corresponds to a small essentially rigid-body displacement of the trimer with respect to the first crystal form. Direct rigid-body refinement from the partially refined structure without molecular replacement yielded effectively the same solution.

The molecular-replacement solutions obtained showed the non-crystallographic molecular threefold axis of the trimer to lie approximately parallel to the *a* axis. This was confirmed by calculation of the self-rotation function using the program *GLRF*, which revealed one peak on the section corresponding to $\kappa = 120^\circ$. This peak lies in the plane defined by the crystallographic *a* and *b* axes at an angle of 18° with respect to *a*. These results pave the way for the full structure determination of the first parasite PNP, opening up new perspectives for an alternative drug-design strategy based on inhibition of the purine-salvage pathway. The fully refined structure will be used for the development of specific SmPNP inhibitors with a view to obtaining alternative treatments for schistosomiasis.

We are grateful to FAPESP and PRONEX (FINEP, CNPq) for financial support and to Astex Technology for providing experimental facilities during the six-month visit of HMP. We also thank José Brandão Neto for excellent technical assistance in the use of the CPr beamline at the LNLS as well as Kátia Barroso for carrying out automated DNA sequencing and Analina F. Valadão for initial directions and assistance on cloning and expression procedures.

References

Brünger, A. T., Adams, P. D., Clore, G. M., DeLano, W. L., Gros, P., Grosse-Kunstleve, R. W., Jiang, J. S., Kuszewski, J., Nilges, M., Pannu, N. S., Read, R. J., Rice, L. M., Simonson, T. & Warren, G. L. (1998). *Acta Cryst.* D**54**, 905–921.

Bzowska, A., Kulikowska, E. & Shugar, D. (2000). *Phamacol. Ther.* **88**, 349–425.

Bzowska, A., Luic, M., Schroder, W., Shugar, D., Saenger, W. & Koellner, G. (1995). *FEBS Lett.* **367**, 214–218.

Carlson, D. A. & Chang, K. P. (1981). *Biochem. Biophys. Res. Commun.* **100**, 1377–1383.

Collaborative Computational Project, Number 4 (1994). *Acta Cryst.* D**50**, 760–763.

Dovey, H. F., McKerrow, J. H. & Wang, C. C. (1984). *Mol. Biochem. Parasitol.* **11**, 157–167.

Franco, G. R., Adams, M. D., Soares, M. B., Simpson, A. J., Venter, J. C. & Pena, S. D. (1995). *Gene*, **152**, 141–147.

Franco, G. R., Valadão, A. F., Azevedo, V. & Rabelo, E. M. L. (2000). *Int. J. Parasitol.* **30**, 453–463.

Kalckar, H. M. (1947). *J. Biol. Chem.* **167**, 429–443.

Kicska, G. A., Tyler, P. C., Evans, G. B., Furneaux, R. H., Schramm, V. L. & Kim, K. (2002). *J. Mol. Biol.* **277**, 3226–3231.

Koellner, G., Luic, M., Shugar, D., Saenger, W. & Bzowska, A. (1997). *J. Mol. Biol.* **265**, 202–216.

Leslie, A. G. W. (1992). *Jnt CCP4/ESF–EAMCB Newsl. Protein Crystallogr.* **26**.

Navaza, J. (1994). *Acta Cryst.* A**50**, 157–163.

Nelson, D. J., LaFon, S. W., Tuttle, J. V., Miller, W. H., Miller, R. L., Krenisky, T. A., Elion, G. B., Berens, R. L. & Marr, J. J. (1979). *J. Biol. Chem.* **254**, 11544–11549.

Otwinowski, Z. & Minor, W. (1997). *Methods Enzymol.* **276**, 307–326.

Senft, A. W. & Crabtree, G. W. (1977). *Biochem. Pharmacol.* **26**, 1847–1855.

Senft, A. W. & Crabtree, G. W. (1983). *Pharmacol. Ther.* **20**, 341–356.

Shuhua, X., Tanner, M., N'Goran, E. K., Utzinger, J., Chollet, J., Bergquist, R., Minggang, C. & Jiang, Z. (2002). *Acta Trop.* **82**, 175–181.

Stoeckler, J. D., Poirot, A. F., Smith, R. M., Parks, E. Jr, Ealick, S. E., Takabayashi, K. & Erion, M. D. (1997). *Biochemistry*, **26**, 11749–11756.

Vagin, A. A. & Teplyakov, A. J. (1997). *J. Appl. Cryst.* **30**, 1022–1025.

Vaguine, A. A., Richelle, J. & Wodak, S. J. (1999). *Acta Cryst.* D**55**, 191–205.

Vuillard, L., Baalbaki, B., Lehmann, M., Nørager, S., Legrand, P. & Roth, M. (1996). *J. Cryst. Growth*, **168**, 150–154.

Williams, S. R., Goddard, J. M. & Martin, D. W. Jr (1984). *Nucleic Acids Res.* **12**, 5779–5787.

World Health Organization. (1999). *Report of the WHO Informal Consultation on Schistosomiasis Control*, WHO/CDS/CPC/SIP/99.2. Geneva: World Health Organization.